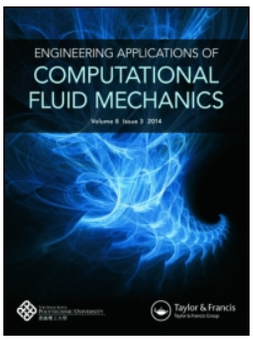

Engineering Applications of Computational Fluid Mechanics

ISSN: 1994-2060 (Print) 1997-003X (Online) Journal homepage: https://www.tandfonline.com/loi/tcfm20

Developing an ANFIS-based swarm concept model for estimating the relative viscosity of nanofluids

Alireza Baghban, Ali Jalali, Mojtaba Shafiee, Mohammad Hossein Ahmadi & Kwok-wing Chau

To cite this article: Alireza Baghban, Ali Jalali, Mojtaba Shafiee, Mohammad Hossein Ahmadi & Kwok-wing Chau (2019) Developing an ANFIS-based swarm concept model for estimating the relative viscosity of nanofluids, Engineering Applications of Computational Fluid Mechanics, 13:1, 26-39, DOI: 10.1080/19942060.2018.1542345

To link to this article: https://doi.org/10.1080/19942060.2018.1542345

Published online: 25 Nov 2018.

ENGINEERING APPLICATIONS OF COMPUTATIONAL FLUID MECHANICS
2018, VOL. 13, NO. 1, 26–39
https://doi.org/10.1080/19942060.2018.1542345

Taylor & Francis
Taylor & Francis Group

Developing an ANFIS-based swarm concept model for estimating the relative viscosity of nanofluids

Alireza Baghban[a], Ali Jalali[b], Mojtaba Shafiee[c], Mohammad Hossein Ahmadi[d] and Kwok-wing Chau[e]

[a]Department of Chemical Engineering, Amirkabir University of Technology (Tehran Polytechnic), Mahshahr, Iran; [b]Department of Chemical Engineering, Amirkabir University of Technology (Tehran Polytechnic), Tehran, Iran; [c]Department of Chemical Engineering, Jundi-Shapur University of Technology, Dezful, Iran; [d]Faculty of Mechanical Engineering, Shahrood University of Technology, Shahrood, Iran; [e]Department of Civil and Environmental Engineering, Hong Kong Polytechnic University, Hong Kong, People's Republic of China

ABSTRACT

Nanofluid viscosity is an important physical property in convective heat transfer phenomena. However, the current theoretical models for nanofluid viscosity prediction are only applicable across a limited range. In this study, 1277 experimental data points of distinct nanofluid relative viscosity (NF-RV) were gathered from a plenary literature review. In order to create a general model, adaptive network-based fuzzy inference system (ANFIS) code was expanded based on the independent variables of temperature, nanoparticle diameter, nanofluid density, volumetric fraction, and viscosity of the base fluid. A statistical analysis of the data for training and testing (with $R^2 = .99997$) demonstrates the accuracy of the model. In addition, the results obtained from ANFIS are compared to similar experimental data and show absolute and maximum average relative deviations of about 0.42 and 6.45%, respectively. Comparisons with other theoretical models from previous research is used to verify the model and prove the prediction capabilities of ANFIS. Consequently, this tool can be of huge value in helping chemists and mechanical and chemical engineers – especially those who are dealing with heat transfer applications by nanofluids – by providing highly accurate predictions of NF-RVs.

ARTICLE HISTORY
Received 31 July 2018
Accepted 27 October 2018

KEYWORDS
nanofluid; viscosity; ANFIS; sensitivity analysis; correlations

1. Introduction

Nanofluids are comprised of a base liquid and uniformly dispersed solid nanoparticles. The word 'nanoparticle' refers to solid particles with a diameter of less than 100 nm. In general, nanofluids have a volumetric fraction of less than 4% nanoparticles (Kamiński & Ossowski, 2014). Nanofluids usually contain TiO_2, Al_2O_3, SiC, SiO_2, and CuO as nanoparticles, and deionized water, water, ethylene glycol, polyalphaolefin, ethanol, or a mixture of ethylene glycol or propylene glycol with water as the base fluid (Mahbubul, Saidur, & Amalina, 2012). Based on recent investigations, nanofluids' thermal conductivity is generally higher than that of the base fluid (Murshed, Leong, & Yang, 2008).

Fluid viscosity is a measure of fluid's internal resistance against flowing, which is the main thermophysical property of fluid – especially in convective thermal applications in the presence of fluid flow. Therefore, fluid viscosity can influence the pumping power needed by altering the friction head and convective heat transfer coefficient. Consequently, because of the complexities of nanofluid hydrodynamics caused by particle–particle collision, a precise model for predicting the viscosity of nanofluids would seem to be essential (Mehrabi, Sharifpur, & Meyer, 2013). In the past 20 years, a number of investigations have been completed on nanofluids, especially on nanofluid synthesis (H. Chen, Ding, & Tan, 2007; L. Chen, Xie, Li, & Yu, 2008) and thermal conductivity (Ahmadi, Alhuyi Nazari, et al., 2018; Ahmadi, Tatar, et al., 2018; Jung, Cho, Lee, & Kang, 2011; S. Lee, Choi, Li, & Eastman, 1999; Shaikh, Lafdi, & Ponnappan, 2007). However, few investigations related to nanofluid relative viscosity (NF-RV) have been carried out, even though this physical property plays a major role in the design of industrial equipment (H. Chen et al., 2007; Duangthongsuk & Wongwises, 2009; J.-H. Lee et al., 2008). Masuda, Ebata, and Teramae (1993) determined the viscosity of an aqueous nanoparticle solution (consisting of Al_2O_3, SiO_2, and TiO_2), while other researchers have evaluated the viscosity of various different nanofluids experimentally (L. Chen et al., 2008; Murshed et al., 2008; Nguyen et al., 2007; Pak & Cho, 1998). In addition, the effects of independent variables like temperature and the shape, diameter, and volumetric fraction of the particles on

CONTACT Mohammad Hossein Ahmadi mohammadhosein.ahmadi@gmail.com; Kwok-wing Chau dr.kwok-wing.chau@polyu.edu.hk

NF-RV have been considered (Mahbubul et al., 2012; Rudyak & Krasnolutskii, 2014; Rudyak, Belkin, & Egorov, 2009).

Modeling could provide an opportunity to formulate a general equation for predicting the viscosity of different nanofluids (Heidari & Ghoreishi, 2013). The Einstein (1906) model ($\mu_{nf} = \mu_{bf}(1 + 2.5\varphi)$) is essentially the first model for predicting NF-RV at a low volumetric fraction of around 0.02 (Eastman, Phillpot, Choi, & Keblinski, 2004). However, for higher volumetric fractions, models based on the power law assumption are superior. For a system of simplified hardened spheres, Krieger and Dougherty's (1959) half-empirical equation makes a good prediction of NF-RV (such as the viscosity ratio of the nanofluid relative to the base fluid). A decade later, Nielsen (1970) proposed a more general equation, while more recently Mehrabi et al. (2013) conducted a comprehensive study on the best correlations for NF-RV. However, model verification is the key point of modeling, which is controlled by simplistic assumptions that are applied to the development of the model.

Lately, heuristic models such as genetic programming, neural networks, and fuzzy logic have generated a lot of attention for their ability to predict thermophysical properties without the need for experimental verification (Aghayari, Maddah, Ahmadi, Yan, & Ghasemi, 2018; Ahmadi, Ahmadi, Mehrpooya, & Rosen, 2015; Ahmadi, Ahmadi, Sadatsakkak, & Feidt, 2015; Ahmadi, Alhuyi Nazari, et al., 2018; Ahmadi, Tatar, et al., 2018; Ahmadi, Sorouri Ghare Aghaj, & Nazeri, 2013; Baghban, Bahadori, Mohammadi, & Behbahaninia, 2017; Baghban, Pourfayaz, et al., 2018; Baghban, Jalali, Mohammadi, & Habibzadeh, 2018; Baghban, Kardani, & Habibzadeh, 2017; Baghban, Mohammadi, & Taleghani, 2017; Faizollahzadeh Ardabili et al., 2018; Fotovatikhah et al., 2018; Ghalamchi, Kasaeian, Ahmadi, & Ghalamchi, 2017; Ghazani, Baghban, Mohammadi, & Habibzadeh, 2018; Kasaeian, Ghalamchi, Ahmadi, & Ghalamchi, 2017; Kazemi et al., 2018; Li, Zhang, & Liu, 2017; Loni, Asli-Ardeh, Ghobadian, Ahmadi, & Bellos, 2018; Pourkiaei, Ahmadi, & Hasheminejad, 2016; Taormina, Chau, & Sivakumar, 1985; Wu & Chau, 2011; S. Zhang & Chau, 2009; Z. Zhang, Li, Chang, Pan, & Luo, 2018). These models, with their data mining approach, are useful for finding complex correlations between noisy and incomplete data. In addition, they are easier to apply than theoretical models (Heidari & Ghoreishi, 2013). Kurt and Kayfeci (2009) developed an artificial neural network (ANN) model for anticipating the effect of temperature and the volumetric fraction and density of nanoparticles on the thermal conductivity of nanofluids based on ethylene glycol and water. Papari, Yousefi, Moghadasi, Karimi, and Campo (2011) present a diffusional neural network (DNN) model for the thermal conductivity of single-wall and multi-wall carbon nanotubes. Nanofluid viscosity prediction is modeled by 182 and 536 experimental data points using a DNN (Yousefi, Karimi, & Papari, 2012) and an adaptive network-based fuzzy inference systems (ANFIS; Mehrabi et al., 2013), respectively. However, these data-driven models are confined to specific nanofluids and a limited range of independent variables.

The final subject of the present investigation is extending a general model, namely ANFIS, for the precise prediction of nanofluid viscosity. Therefore, experimental data for NF-RV were collected from

Table 1. General specifications of the present data set.

Parameters	Range
Temperature	−35.0–71.2°C
Nanoparticle diameter	7–190 nm
Nanoparticle volumetric fraction	0–9%
Nanoparticle density	2650–6310 kg m^{-3}
Base fluid viscosity	0.394–452.599 cp
Nanofluid relative viscosity	0.560–9.776

Table 2. Detailed analysis of the present data set.

Nanoparticle	Base fluid	No. of data points	References
TiO_2	DI water	3	Murshed et al. (2008)
Al_2O_3	DI water	3	Murshed et al. (2008)
Al_2O_3	Water	499	Nguyen et al. (2007); Lee et al. (2008); Tavman, Turgut, Chirtoc, Schuchmann, and Tavman (2008); Chandrasekar, Suresh, and Chandra Bose (2010); Mehrabi et al. (2013); Meybodi et al. (2016)
SiC	DI water	4	Lee et al. (2011)
TiO_2	Water	13	Duangthongsuk and Wongwises (2009)
Al_2O_3	Transformer oil	15	Singh and Kundan (2013)
SiO_2	DI water	50	Zhao et al. (2009)
TiO_2	Ethylene glycol	135	Chen et al. (2007)
SiO_2	Ethanol	16	Chevalier, Tillement, and Ayela (2007)
CuO	Water	291	Nguyen et al. (2007); Pastoriza-Gallego et al. (2011); Mehrabi et al. (2013); Meybodi, Naseri, Shokrollahi, and Daryasafar (2015); Meybodi et al. (2016)
CuO	Propylene glycol and water, 30:70	34	Naik and Sundar (2011)
CuO	Propylene glycol and water, 60:40	72	Namburu, Kulkarni, Misra, and Das (2007); Kulkarni, Das, and Vajjha (2009)
SiO_2	Water	19	Tavman et al. (2008)
SiO_2	Transformer oil	6	Jamshidi et al. (2012)
SiO_2	Ethylene glycol and water, 25:75	7	Jamshidi et al. (2012)
SiO_2	Ethylene glycol and water, 50:50	30	Jamshidi et al. (2012)
SiO_2	Ethylene glycol	47	Rudyak et al. (2013)
Al_2O_3	R1 1 refrigerant	13	Singh and Kundan (2013)
Al_2O_3	Polyalphaolefins	20	Zhou, Ni, and Funfschilling (2010)

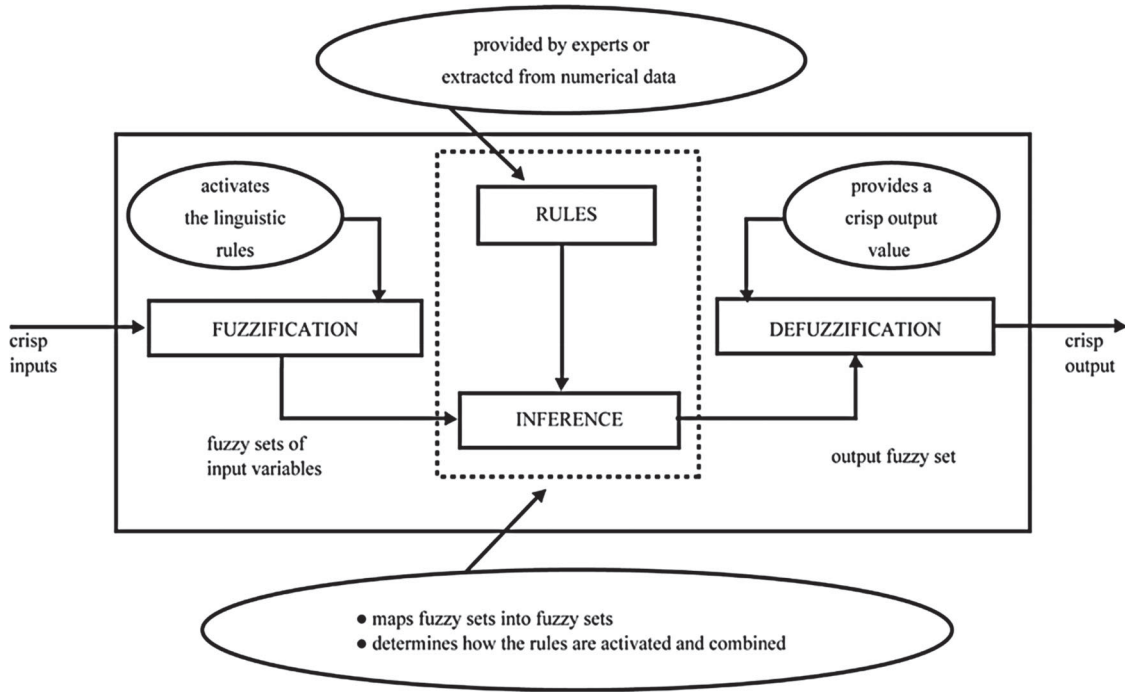

Figure 1. Schematic structure of a fuzzy inference system (FIS).

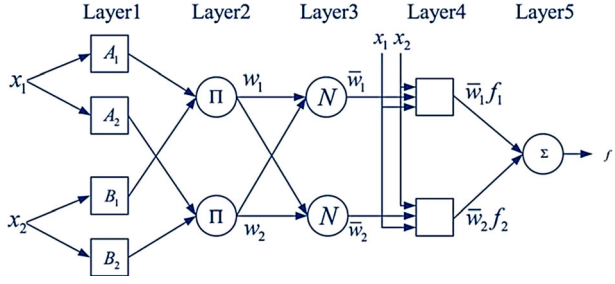

Figure 2. Structure of an ANFIS model with two input parameters.

verified studies across a wide range of conditions. Lastly, the results of the proposed ANFIS model are verified using the theoretical models of Einstein (1906), H. Chen et al. (2007), Maïga, Nguyen, Galanis, and Roy (2004), Batchelor (1977), Brinkman (1952), and Hosseini, Moghadassi, and Henneke (2010). In addition, the suggested ANFIS model is checked with new correlations.

2. Data sets

There are a number of experimental investigations of NF-RV (H. Chen et al., 2007; Duangthongsuk & Wongwises, 2009; J.-H. Lee et al., 2008; S. W. Lee, Park, Kang, Bang, & Kim, 2011; Murshed et al., 2008; Singh & Kundan, 2013; Zhao, Luo, Ni, & Cen, 2009). The independent variables in these studies include temperature, volume concentration, nanoparticle diameter, shape, and aspect ratio, and inter-particle spacing. In addition, the effects of settling time, fluid density, fluid polarity, etc. on NF-RV have also been investigated experimentally (Meyer, Nwosu, Sharifpur, & Ntumba, 2012). In previous studies, three independent variables such as temperature, nanoparticle diameter, and nanoparticle volumetric fraction were chosen as the model inputs. However, these models are only carried out for specific nanofluids, so they are not universal and applicatory to all nanofluids (Mehrabi et al., 2013). In the present study, these three variables are also applied; however, other input parameters are introduced in order to generalize the model to different types of nanoparticle. The fourth input parameter can be the molecular weight or bulk density of the nanoparticles. It is inferred that the ANFIS model's ability can be improved by including the nanoparticle bulk density as another input parameter. The fifth input parameter is the viscosity of the base fluid. A detailed analysis and specification of the 1277 data points for the NF-RVs across a wide range of different input parameters is shown in Tables 1 and 2. These data points are classified into two groups, the first of which was used for training the system and the second of which was used for verifying the model; three quarters of the data points were used as training data and the remainder were used as testing data.

3. Theory

3.1. ANFIS model

Figure 1 presents the schematic structure of fuzzy inference system (FIS) processing, which is comprised of four

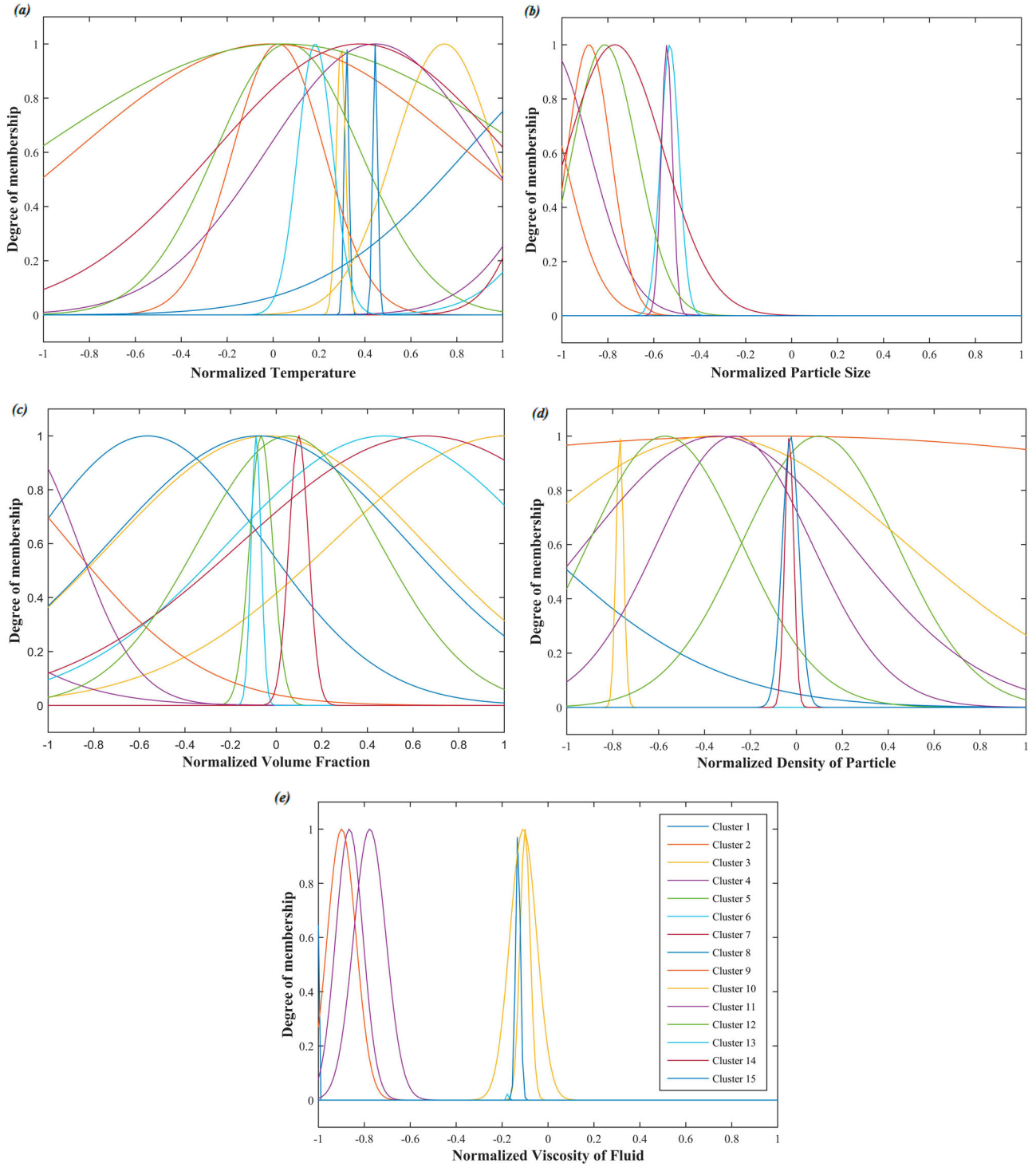

Figure 3. The final status of the MFs after training using the PSO method for input parameters: (a) temperature; (b) particle diameter; (c) volumetric fraction; (d) particle density; (e) fluid viscosity.

sections: the knowledge base, the inference engine, fuzzification inference, and defuzzification (Jang, 1993). The ANFIS model has diverse interconnected nodes in its structure. A number of these nodes have adaptive sections, which means that their output is limited by setting the value for that node.

3.2. ANFIS structure

For the FIS, x_1 and x_2 are assumed for the importing variables and y is assumed for the exporting variable. Then, principles are formed as conditional statements (e.g., if $x_1 = A$ and $x_2 = B$ then $y = f(x_1, x_2)$), in which A and B are considered fuzzy sets (FSs) and y is named a

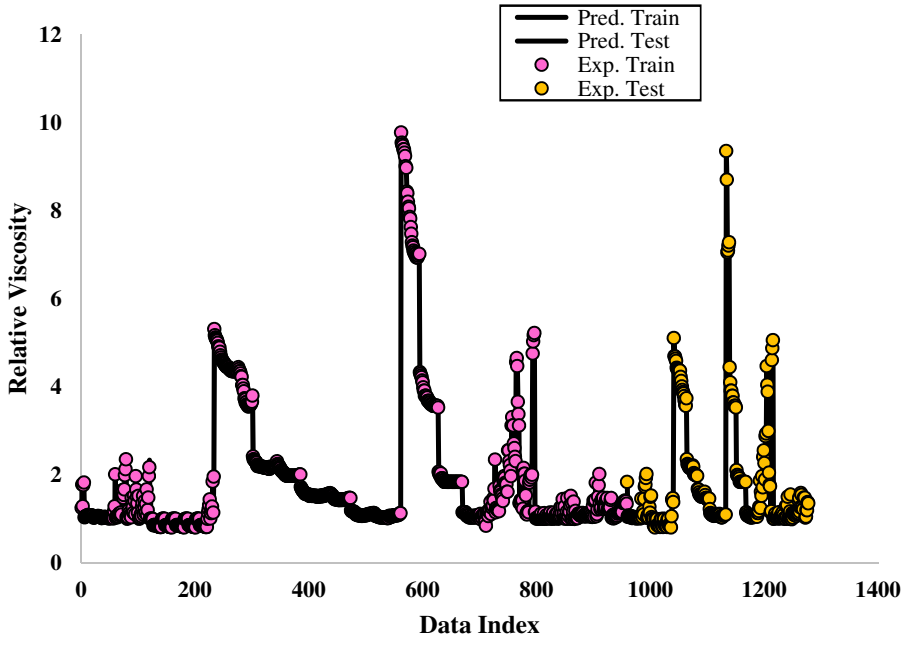

Figure 4. Predicted and experimental NF-RV values.

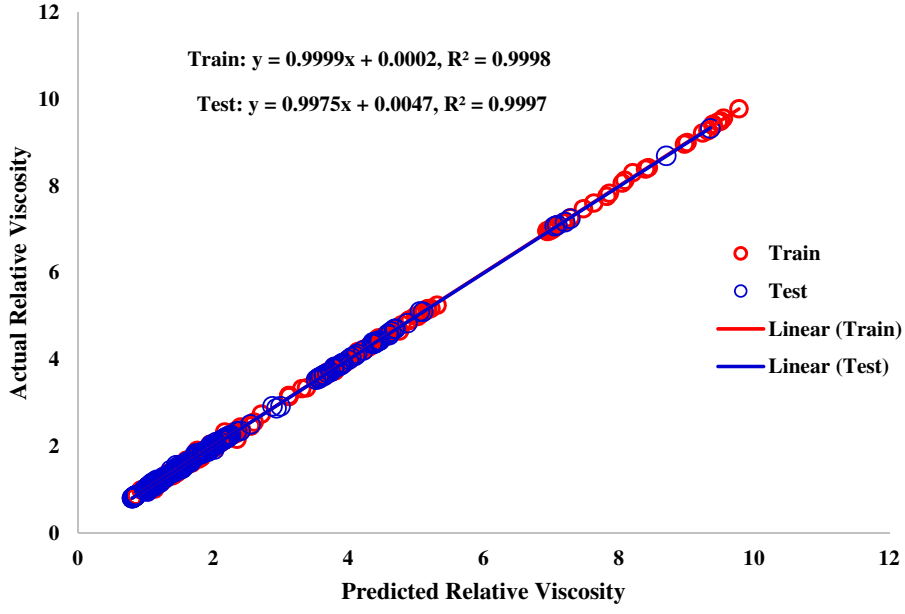

Figure 5. Cross plot of the predictions of the PSO-ANFIS model.

crisp function (CF). CFs can be any function (generally of a polynomial form) that is capable of giving an output under specific conditions (Jang, 1993).

In the case of assuming the status of $f(x_1, x_2) =$ cte, a Sugeno-type fuzzy model with an order of zero is obtained. For a particular condition, any available law will follow the similar resultant section. In the case of assuming a first-order polynomial for $f(x_1, x_2)$, a first-order Sugeno FIS is encountered.

The method proposed in Takagi and Sugeno (1993) has become the most popular choice for ANFIS development; it has been used in various studies across different fields due to its excellent efficiency. Therefore, in the present study, a Takagi–Sugeno FIS is applied to the prediction of NF-RV values.

For the assumption of two first-order polynomials, laws of the Takagi–Sugeno type can be written as follows (Takagi & Sugeno, 1993):

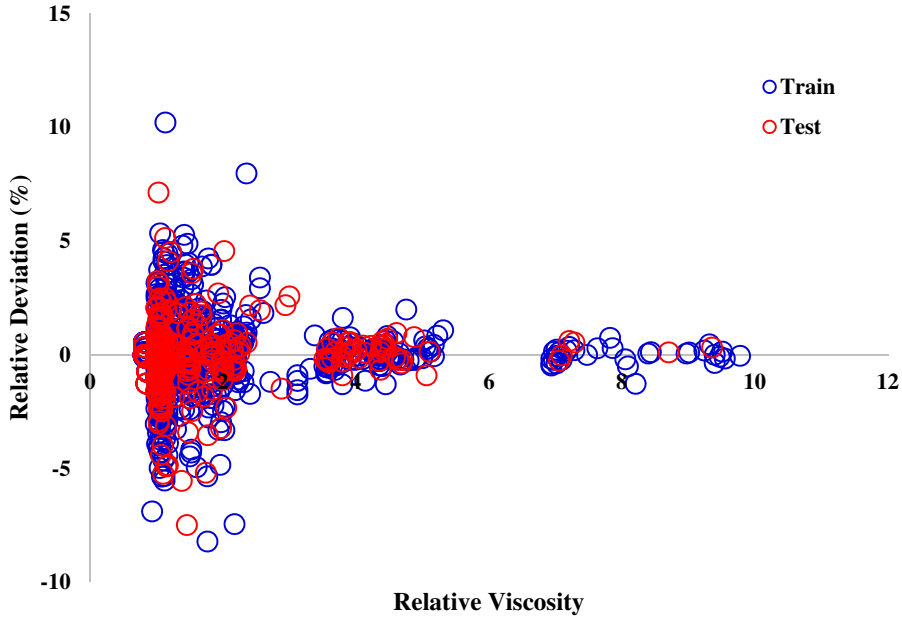

Figure 6. Relative error plot of the outcomes of the PSO-ANFIS model.

Table 3. Calculated statistical parameters for the PSO-ANFIS model.

Dataset	R^2	AARD	STD	RMSE
Training	.999	.977	.018	.023
Testing	.999	.994	.017	.022

Note: AARD = average absolute relative deviation; RMSE = root mean square error; STD = standard.

Law I: If (x_1 is A_1) and (x_2 is B_1) then $f_1 = p_1x_1 + q_1x_2 + r_1$.

Law I: If (x_1 is A_2) and (x_2 is B_2) then $f_2 = p_2x_1 + q_2x_2 + r_2$.

Then a weighting-based averaging method is used for calculating the average of different existing laws' outputs, which is assumed as an output for the model. This structure is described schematically using squares and circles in Figure 2, which represent adaptive and fixed nodes, respectively. There are five layers that nodes can be placed inside, and it can be seen that the nodes in each layer act in the same way (Baghban, Bahadori, et al., 2017; Baghban, Kardani, & Habibzadeh, 2017; Baghban, Mohammadi, & Taleghani, 2017).

In Layer 1, the nodes that are connected to inputs operate certain membership functions (MFs). Gaussian-type memberships functions, as formulated below, are the most common type of MF:

$$O_i^1 = \beta(X) = \exp\left(-\frac{1}{2}\frac{(X-Z)^2}{\sigma^2}\right), \tag{1}$$

where O is the layer output, σ is the variance parameter, and Z is the Gaussian MF center. The suggested model optimizes these parameters in order to improve accuracy. In Layer 2, the following equation is applied in order to evaluate the antecedent's condition consistency and the reliability of the model:

$$O_i^2 = W_i = \beta_{Ai}(X).\beta_{Bi}(X). \tag{2}$$

Layer 3 applies the following equation in order to normalize the values of W_i predicted in the prior step:

$$O_i^3 = \frac{W_i}{\sum_i W_i}. \tag{3}$$

Table 4. Some available models for the prediction of nanofluid viscosity.

Model	Correlation	Remarks
Einstein (1906)	$\mu_{nf}(CP) = \mu_{bf}(1 + 2.5\varphi)$	Spherical particles, low particle volumetric fraction $\varphi < 0.02$
Maïga et al. (2004)	$\mu_{nf}(CP) = \mu_{bf}(1 + 7.3\varphi + 123\varphi^2)$	
Batchelor (1977)	$\mu_{nf}(CP) = \mu_{bf}(1 + 2.5\varphi + 6.5\varphi^2)$	
Chen et al. (2007)	$\mu_{nf}(CP) = \mu_{bf}(1 + 10.6\varphi + 10.6\varphi^2)$	
Hosseini et al. (2010)	$\mu_{nf}(CP) = \mu_{bf}\exp\left(m + \alpha\left(\frac{T}{T_0}\right) + \beta(\varphi) + \gamma\left(\frac{d_p}{1+R}\right)\right)$ $\alpha = -0.485, \beta = 14.94, \gamma = 0.0105$ $m = 0.72, T_0 = 20^\circ C, R = 1nm$	For Al_2O_3/H_2O
Brinkman (1952)	$\mu_{nf}(CP) = \mu_{bf}(1-\varphi)^{2.5}$	

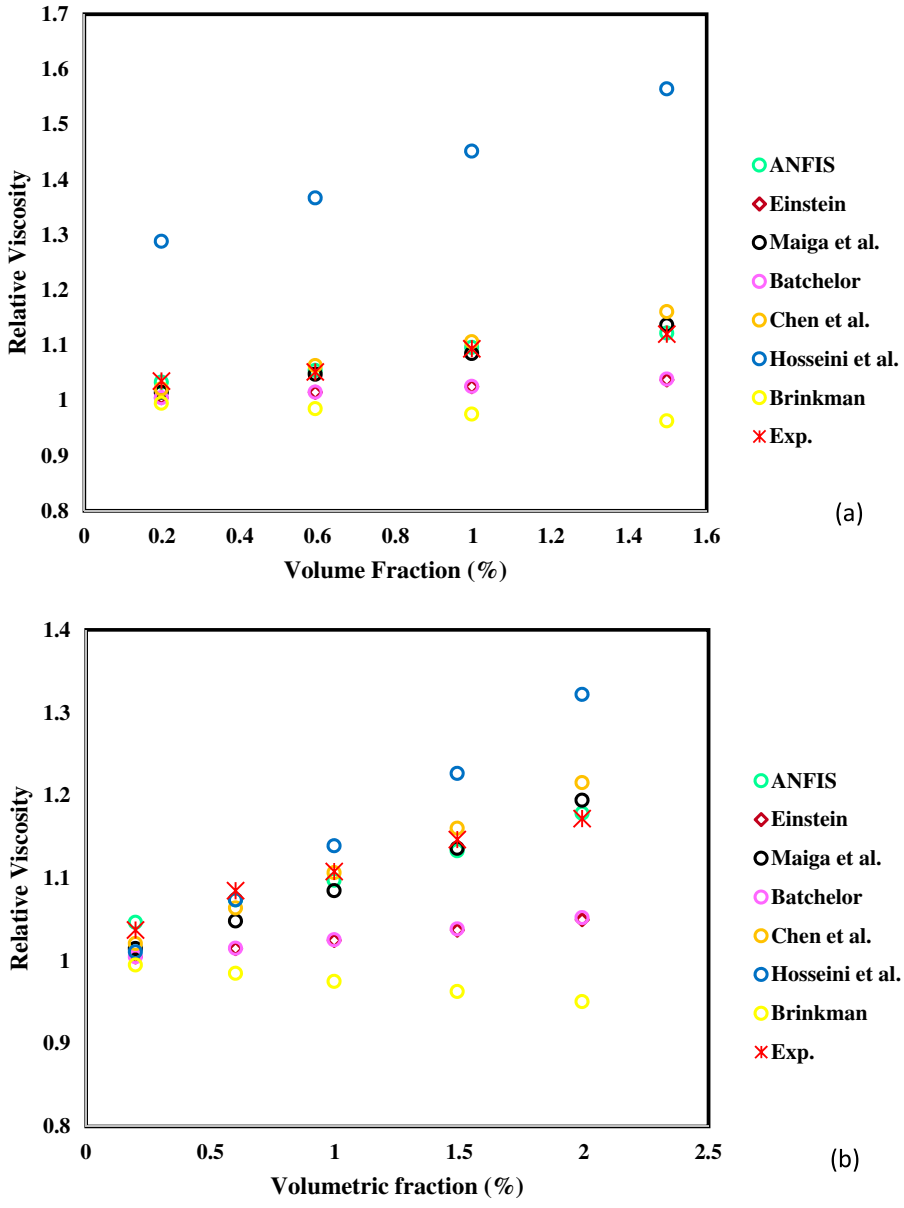

Figure 7. Comparison of the predicted NF-RVs with the experimental data for: (a) TiO_2–water, $t = 25$°C, nanoparticle diameter = 21 nm; (b) TiO_2–water, $t = 35$°C, nanoparticle diameter = 21 nm (Duangthongsuk & Wongwises, 2009).

Layer 4 is responsible for specifying the output linguistic terms, using the following equation to specify the result level:

$$O_i^4 = \overline{W_i} f_i = \overline{W_i}(m_i X_1 + n_i X_2 + r_i). \quad (4)$$

In order to optimize the efficiency, the linear parameters m_i, n_i, and r_i are improved by ANFIS. Finally, in Layer 5 all laws that are connected to an output parameter are considered by the following equation:

$$O_i^5 = Y = \sum_i \overline{W_i} f_i = \overline{W_1} f_1 + \overline{W_2} f_2 = \frac{\sum_i W_i f_i}{\sum_i W_i}. \quad (5)$$

4. Model development

In the first stage of the development of the model, an initial structure for the FIS was created using the MATLAB 2014 genfis function. The Takagi–Sugeno–Kang type of FIS can be obtained using various methods, including grid partition, the lookup table method, fuzzy c-means, and the subtractive clustering method. In the proposed ANFIS model, the subtractive clustering method and Gaussian MFs were applied to the initial structure and the MF type, respectively. In addition, 15 clusters were used; therefore, based on the input and MF parameters, a total of 180 parameters existed for tuning. The FIS structure, once created, needed to be trained to improve

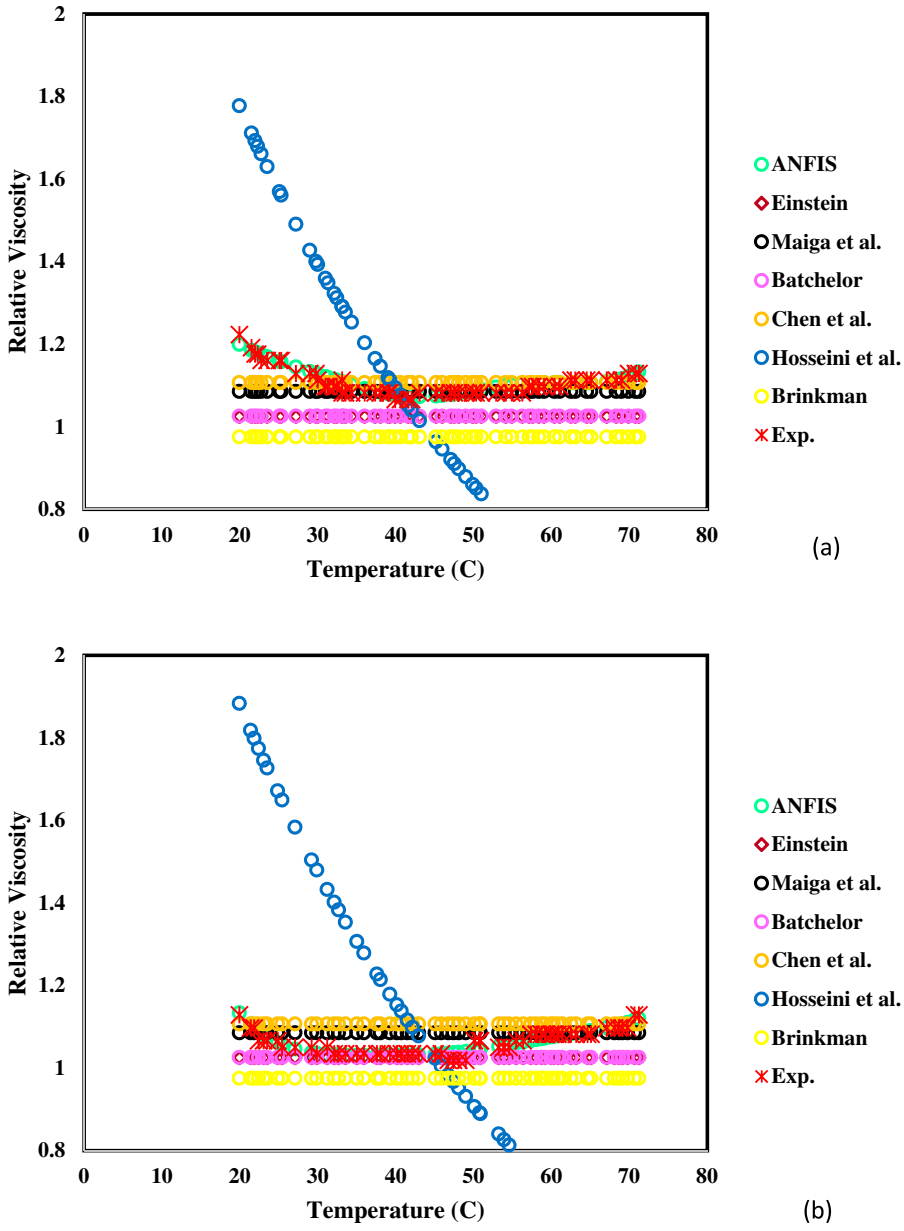

Figure 8. Comparison of the predicted NF-RVs with the experimental data for: (a) Al_2O_3–water, nanoparticle diameter = 36 nm, particle volumetric fraction = 1%; (b) Al_2O_3–water, nanoparticle diameter = 47 nm, particle volumetric fraction = 1% (Nguyen et al., 2007).

the model's efficiency. In the present study, FIS training was undertaken using the particle swarm optimization (PSO) method in MATLAB 2014. The improved MFs of the trained FIS are demonstrated in Figure 3. The optimal structure was obtained at an iteration of 1200 and a population size of 80.

5. Results and discussion

5.1. Model verification

Verification of the proposed PSO-ANFIS model was carried out using both statistical and graphical methods. The experimental and estimated values are presented in Figure 4 for both the training and testing data sets, and it can be seen that they are in good agreement. A cross plot of the model, which compares the predicted NF-RV data with the experimental values, is shown in Figure 5. It can be seen that the data points are spread close to the $y = x$ line, which means that the predicted data exhibits adequate consistency and good agreement with the target NF-RV values. The relative error of the model predictions compared to the target NF-RV data is shown in Figure 6. It can be seen that most of the errors are grouped close to the zero lines, which proves the accuracy and reliability of the proposed model. It is also notable that the maximum

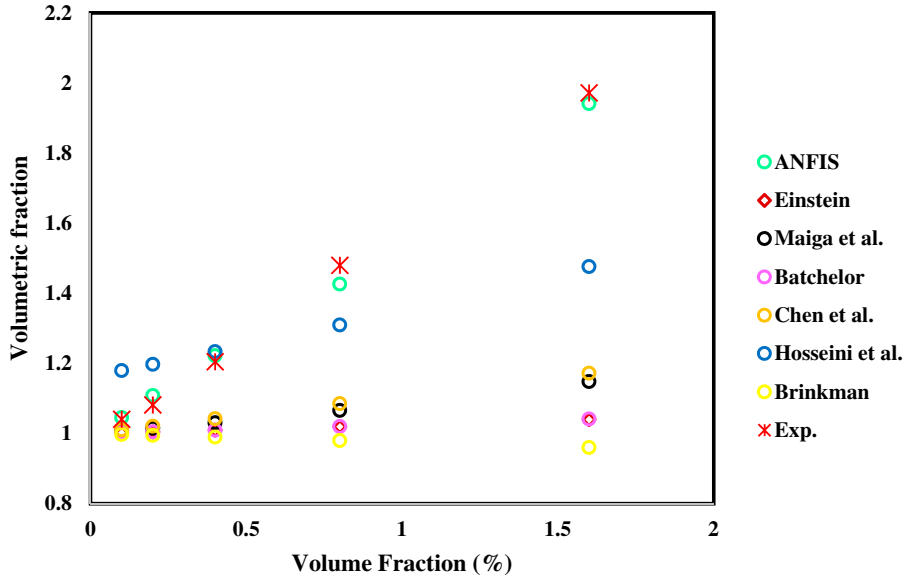

Figure 9. Comparison between the NF-RV data predicted by different models and the experimental data for SiO2–DI water, $t = 25°C$, nanoparticle diameter = 7 nm (Zhao et al., 2009).

model error is less than 10%. Four statistical parameters for assessing the accuracy of the proposed model are also introduced as follows:

$$R^2 = 1 - \frac{\sum_{i=1}^{N} (\rho_{\text{pred}}(i) - \rho_{\text{Exp}(i)})^2}{\sum_{i=1}^{N} (\rho_{\text{pred}}(i) - \bar{\rho}_{\text{Exp}(i)})^2}, \quad (6)$$

$$\%\text{AARD} = \frac{100}{N} \sum_{i=1}^{N} \frac{(\rho_{\text{pred}}(i) - \rho_{\text{Exp}}(i))}{\rho_{\text{Exp}(i)}}, \quad (7)$$

$$\text{MSE} = \left(\frac{\sum_{i=1}^{N} (\rho_{\text{pred}}(i) - \rho_{\text{Exp}}(i))^2}{N} \right)^{0.5}, \quad (8)$$

$$\text{STD} = \sum_{i=1}^{n} \left(\frac{(\rho_{\text{pred}}(i) - \bar{\rho}_{\text{Exp}}(i))^2}{N} \right)^{0.5}. \quad (9)$$

Table 3 shows the values of these parameters for the training and testing data sets. The data points were randomly divided into training and testing classes. It is clear that the proposed model has a low average absolute relative deviation (AARD) value and a relatively high R^2 value, which confirms the model's applicability and reliability.

5.2. Comparative evaluations

The proposed ANFIS model was developed to calculate the NF-RVs, which are listed in Table 2. Several models from the literature (see Table 4) were selected for comparison with the results generated by the proposed model.

The predicted NF-RVs of TiO_2 and water with a particle diameter of 21 nm at room temperature as a function of volumetric fraction are compared to the experimental results in Figure 7(a) (Duangthongsuk & Wongwises, 2009). It can be seen that the NF-RV predicted by the ANFIS model is in good agreement with the experimental data. In addition, it seems that in the range of 0.0 to 2.5% the more the volumetric fraction of the particle the more the NF-RV values. It should be noted that in previous models such as those presented in Einstein (1906), H. Chen et al. (2007), Batchelor (1977), Maïga et al. (2004), and Brinkman (1952), the NF-RV is investigated as a function of the viscosity of the base fluid and the volumetric fraction. Thus, the viscosity predicted by these models is fixed against time changes. The trend of the NF-RVs calculated by previous models is steady versus temperature variations. A comparison of the experimental data and the calculated NF-RVs of TiO_2 and water nanofluid versus the particle volumetric fraction is presented in Figure 7(b).

The experimental data are compared to the calculated NF-RVs for Al_2O_3 and water with a particle diameter of 36 nm and a volumetric fraction of 1% versus temperature in Figure 8(a) (Nguyen et al., 2007). The NF-RVs predicted by the ANFIS model are in very good agreement with the experimental data. The results of the other models are in reasonable to good agreement with the experimental data, with the exception of the model of Hosseini et al. (2010), which is greatly affected by the temperature and varies considerably from the experimental results. The NF-RVs for Al_2O_3 and water with a particle diameter of 47 nm at room temperature against particle volumetric

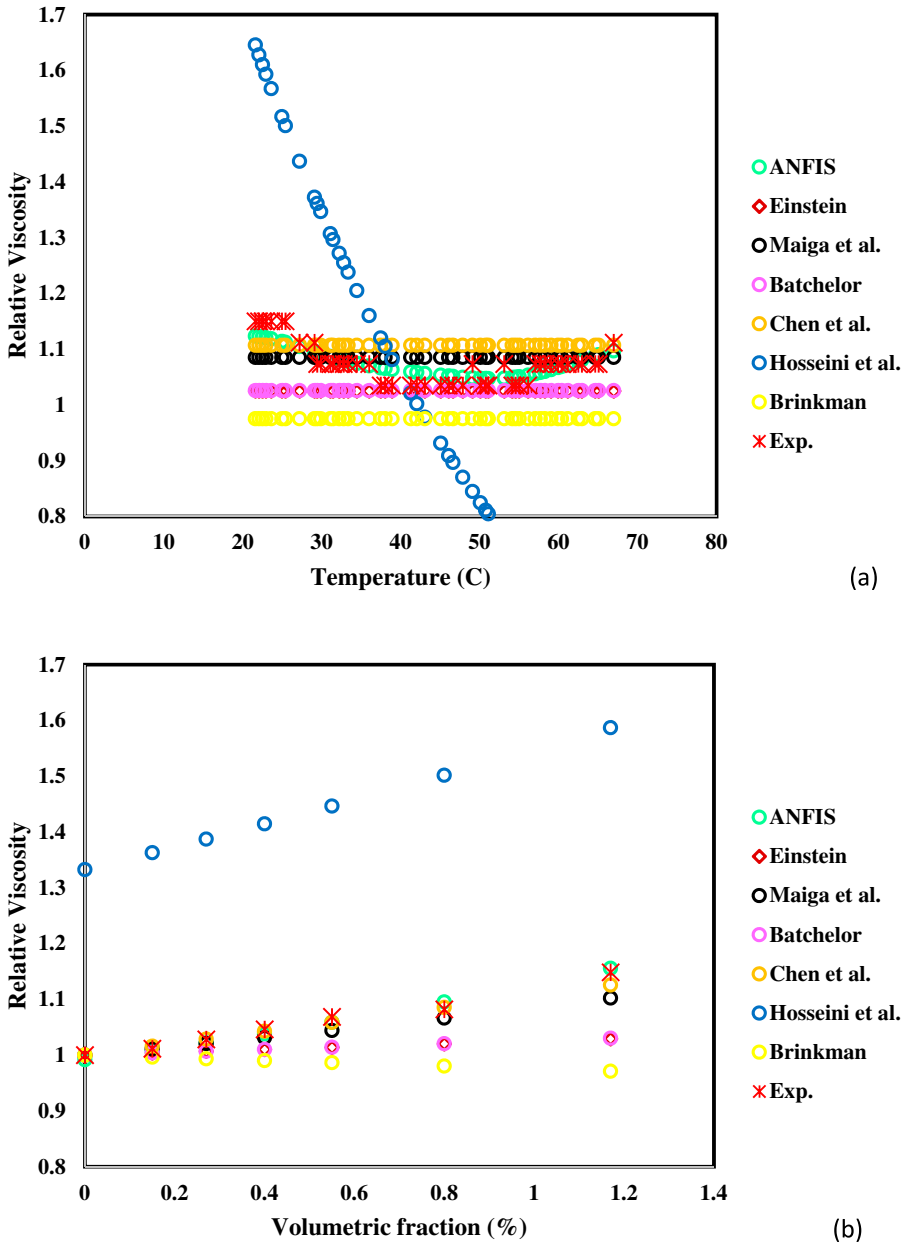

Figure 10. Comparison of the predicted NF-RVs with the experimental data for: (a) CuO–water, nanoparticle diameter = 29 nm, particle volumetric fraction = 1% (Nguyen et al., 2007); (b) CuO–water, nanoparticle diameter = 33 nm, t = 25°C (Pastoriza-Gallego et al., 2011).

fraction are illustrated in Figure 8(b) (Jamshidi, Farhadi, Ganji, & Sedighi, 2012). Ascending attitude in all the theoretical models is observed; however, the ANFIS model shows the best agreement with the experimental data.

The experimental data are compared to the calculated NF-RVs for SiO_2 and deionized water with a particle diameter of 7 nm at room temperature versus the nanoparticle volumetric fraction in Figure 9 (Zhao et al., 2009). It is clear that the ANFIS calculations are in very good agreement with the experimental data, and compare favorably with the results of the other models.

The experimental data are compared to the calculated NF-RVs for CuO and water with a particle diameter of 29 nm and a volumetric fraction of 1% versus temperature in Figure 10(a) (Nguyen et al., 2007). It can be seen that only the ANFIS model has a very good fit to the experimental data compared to the other models. The calculated NF-RVs of CuO and water versus the volumetric fraction are compared to the experimental data in Figure 10(b) (Pastoriza-Gallego, Casanova, Legido, & Piñeiro, 2011). Again, the ANFIS model is in very good accordance with the experimental data, and compares favorably with the other models. Figures 7 to 10 show

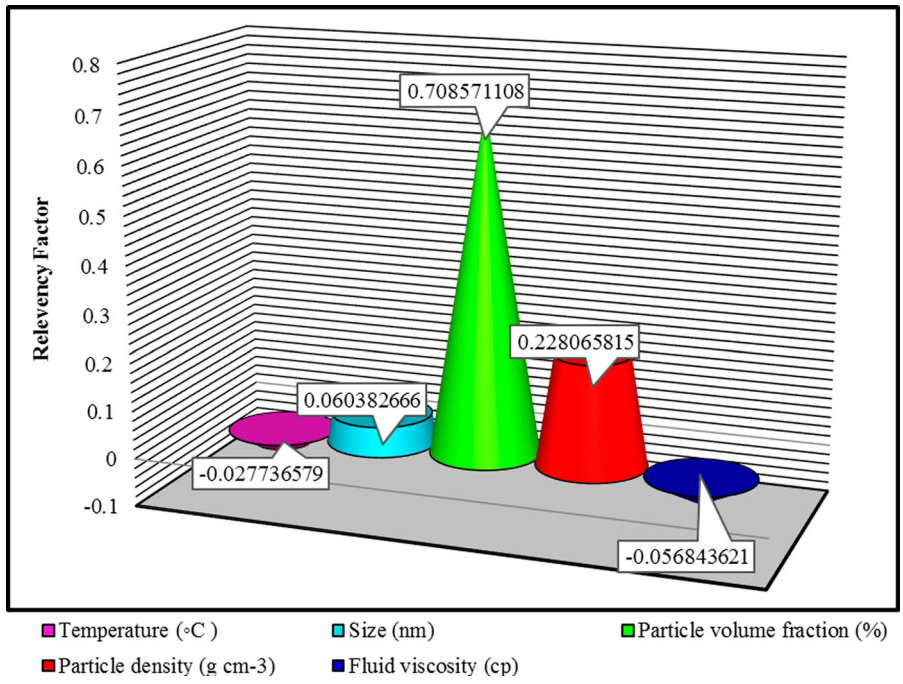

Figure 11. Results of the sensitivity analysis conducted on the ANFIS model.

that the predictions of the proposed ANFIS model are in very good agreement with the experimental data for all the NF-RV values. This demonstrates that the proposed model is a flexible and accurate tool for modeling complex non-linear dependencies between a number of parameters without predefining the correlation structures.

5.3. Sensitivity analysis

The proposed ANFIS model can potentially provide good dependency between the inputs and the output. In order to investigate how the inputs affect the output, a sensitivity analysis was undertaken. The most effective input can be recognized by the relevance factor r, which is in the range of -1 to $+1$ and is stated by the following equation (Hosseinzadeh & Hemmati-Sarapardeh, 2014):

$$r = \frac{\sum_{i=1}^{n}(X_{k,i} - \overline{X_k})(Y_i - \bar{Y})}{\sqrt{\sum_{i=1}^{n}(X_{k,i} - \overline{X_k})^2 \sum_{i}^{n}(Y_i - \bar{Y})^2}}, \qquad (10)$$

where $X_{k,i}$ is the ith importing parameter, Y_i is the ith exporting value, $\overline{X_k}$ is the average value of the kth input, $\bar{Y}$ is the average value of exporting parameter, and n is the number of sets. The absolute value of r has a direct relation on the output. As can be seen in Figure 11, the NF-RV shows a straight dependency on the particle diameter, the particle volumetric fraction, and the particle density, and an opposite dependency on the temperature and the viscosity of the base fluid. In addition, the particle volumetric fraction is the most effective input variable by a 0.71 relation factor and the temperature is the most ineffective parameter by a -0.023 relation factor.

6. Conclusion

In this study, a generalizable and precise model for predicting NF-RVs is proposed using ANFIS. The input variables consist of the temperature, base fluid viscosity, and nanoparticle volumetric fraction, diameter, and density. The ANFIS model results were compared to experimental training and testing data, and the validity and sufficiency of the proposed model for a wide range of input variables was affirmed by an AARD value of 0.98% and an R^2 value of .9997. In addition, the proposed model results were compared to literature correlations and existing theoretical models, and it was shown that the proposed model generates accurate and reliable results compared to prior modeling of NF-RVs. Consequently, this tool is potentially of huge value, as it can provide chemists and mechanical and chemical engineers – especially those who deal with heat transfer applications by nanofluids – with a tool for estimating NF-RVs with a high degree of accuracy. In future work, other approaches such as using different types of ANNs and support vector machines (SVMs) optimized using different algorithms can be implemented and compared with the results generated by the ANFIS model proposed in the present study.

Disclosure statement

No potential conflict of interest was reported by the authors.

References

Aghayari, R., Maddah, H., Ahmadi, M., Yan, W.-M., & Ghasemi, N. (2018). Measurement and artificial neural network modeling of electrical conductivity of CuO/glycerol nanofluids at various thermal and concentration conditions. *Energies*, *11*(5), Article no. 1190.

Ahmadi, M. H., Ahmadi, M. A., Mehrpooya, M., & Rosen, M. (2015). Using GMDH neural networks to model the power and torque of a Stirling engine. *Sustainability*, *7*(2), 2243–2255.

Ahmadi, M. H., Ahmadi, M. A., Sadatsakkak, S. A., & Feidt, M. (2015). Connectionist intelligent model estimates output power and torque of Stirling engine. *Renewable and Sustainable Energy Reviews*, *50*, 871–883.

Ahmadi, M. H., Alhuyi Nazari, M., Ghasempour, R., Madah, H., Shafii, M. B., & Ahmadi, M. A. (2018). Thermal conductivity ratio prediction of Al2O3/water nanofluid by applying connectionist methods. *Colloids and Surfaces A: Physicochemical and Engineering Aspects*, *541*, 154–164.

Ahmadi, M. H., Sorouri Ghare Aghaj, S., & Nazeri, A. (2013). Prediction of power in solar Stirling heat engine by using neural network based on hybrid genetic algorithm and particle swarm optimization. *Neural Computing and Applications*, *22*(6), 1141–1150.

Ahmadi, M. H., Tatar, A., Alhuyi Nazari, M., Ghasempour, R., Chamkha, A. J., & Yan, W.-M. (2018). Applicability of connectionist methods to predict thermal resistance of pulsating heat pipes with ethanol by using neural networks. *International Journal of Heat and Mass Transfer*, *126*, 1079–1086.

Baghban, A., Bahadori, A., Mohammadi, A. H., & Behbahaninia, A. (2017). Prediction of CO_2 loading capacities of aqueous solutions of absorbents using different computational schemes. *International Journal of Greenhouse Gas Control*, *57*, 143–161.

Baghban, A., Jalali, A., Mohammadi, A. H., & Habibzadeh, S. (2018). Efficient modeling of drug solubility in supercritical carbon dioxide. *The Journal of Supercritical Fluids*, *133*, 466–478.

Baghban, A., Kardani, M. N., & Habibzadeh, S. (2017). Prediction viscosity of ionic liquids using a hybrid LSSVM and group contribution method. *Journal of Molecular Liquids*, *236*, 452–464.

Baghban, A., Mohammadi, A. H., & Taleghani, M. S. (2017). Rigorous modeling of CO_2 equilibrium absorption in ionic liquids. *International Journal of Greenhouse Gas Control*, *58*, 19–41.

Baghban, A., Pourfayaz, F., Ahmadi, M. H., Kasaeian, A., Pourkiaei, S. M., & Lorenzini, G. (2018). Connectionist intelligent model estimates of convective heat transfer coefficient of nanofluids in circular cross-sectional channels. *Journal of Thermal Analysis and Calorimetry*, *132*(2), 1213–1239.

Batchelor, G. (1977). The effect of Brownian motion on the bulk stress in a suspension of spherical particles. *Journal of Fluid Mechanics*, *83*(1), 97–117.

Brinkman, H. (1952). The viscosity of concentrated suspensions and solutions. *The Journal of Chemical Physics*, *20*(4), 571–571.

Chandrasekar, M., Suresh, S., & Chandra Bose, A. (2010). Experimental investigations and theoretical determination of thermal conductivity and viscosity of Al_2O_3/water nanofluid. *Experimental Thermal and Fluid Science*, *34*(2), 210–216.

Chen, H., Ding, Y., & Tan, C. (2007). Rheological behaviour of nanofluids. *New Journal of Physics*, *9*(10) 367.

Chen, L., Xie, H., Li, Y., & Yu, W. (2008). Nanofluids containing carbon nanotubes treated by mechanochemical reaction. *Thermochimica Acta*, *477*(1–2), 21–24.

Chevalier, J., Tillement, O., & Ayela, F. (2007). Rheological properties of nanofluids flowing through microchannels. *Applied Physics Letters*, *91*(23), 233103.

Duangthongsuk, W., & Wongwises, S. (2009). Measurement of temperature-dependent thermal conductivity and viscosity of TiO_2–water nanofluids. *Experimental Thermal and Fluid Science*, *33*(4), 706–714.

Eastman, J. A., Phillpot, S. R., Choi, S. U. S., & Keblinski, P. (2004). Thermal transport in nanofluids. *Annual Review of Materials Research*, *34*, 219–246.

Einstein, A. (1906). Eine neue bestimmung der moleküldimensionen. *Annalen der Physik*, *324*(2), 289–306.

Faizollahzadeh Ardabili, S., Najafi, B., Shamshirband, S., Minaei Bidgoli, B., Deo, R. C., & Chau, K.-W. (2018). Computational intelligence approach for modeling hydrogen production: A review. *Engineering Applications of Computational Fluid Mechanics*, *12*(1), 438–458.

Fotovatikhah, F., Herrera, M., Shamshirband, S., Chau, K.-W., Faizollahzadeh Ardabili, S., & Piran, M. J. (2018). Survey of computational intelligence as basis to big flood management: Challenges, research directions and future work. *Engineering Applications of Computational Fluid Mechanics*, *12*(1), 411–437.

Ghalamchi, M., Kasaeian, A., Ahmadi, M. H., & Ghalamchi, M. (2017). Evolving ICA and HGAPSO algorithms for prediction of outlet temperatures of constructed solar chimney. *International Journal of Low-Carbon Technologies*, *12*(2), 84–95.

Ghazani, S. H. H. N., Baghban, A., Mohammadi, A. H., & Habibzadeh, S. (2018). Absorption of CO_2-rich gaseous mixtures in ionic liquids: A computational study. *The Journal of Supercritical Fluids*, *133*, 455–465.

Heidari, E., & Ghoreishi, S. (2013). Prediction of supercritical extraction recovery of EGCG using hybrid of adaptive neuro-fuzzy inference system and mathematical model. *The Journal of Supercritical Fluids*, *82*, 158–167.

Hosseini, S. M., Moghadassi, A. R., & Henneke, D. E. (2010). A new dimensionless group model for determining the viscosity of nanofluids. *Journal of Thermal Analysis and Calorimetry*, *100*(3), 873–877.

Hosseinzadeh, M., & Hemmati-Sarapardeh, A. (2014). Toward a predictive model for estimating viscosity of ternary mixtures containing ionic liquids. *Journal of Molecular Liquids*, *200*, 340–348.

Jamshidi, N., Farhadi, M., Ganji, D. D., & Sedighi, K. (2012). Experimental investigation on the viscosity of nanofluids. *International Journal of Engineering. Transactions B: Applications*, *25*(3), 201–209.

Jang, J.-S. (1993). ANFIS: Adaptive network-based fuzzy inference system. *IEEE Transactions on Systems, Man, and Cybernetics*, *23*(3), 665–685.

Jung, J.-Y., Cho, C., Lee, W. H., & Kang, Y. T. (2011). Thermal conductivity measurement and characterization of binary

nanofluids. *International Journal of Heat and Mass Transfer*, *54*(9–10), 1728–1733.
Kamiński, M., & Ossowski, R. L. (2014). Prediction of the effective parameters of the nanofluids using the generalized stochastic perturbation method. *Physica A: Statistical Mechanics and its Applications*, *393*, 10–22.
Kasaeian, A., Ghalamchi, M., Ahmadi, M. H., & Ghalamchi, M. (2017). GMDH algorithm for modeling the outlet temperatures of a solar chimney based on the ambient temperature. *Mechanics & Industry*, *18*(2), 216.
Kazemi, S., Minaei Bidgoli, B., Shamshirband, S., Karimi, S. M., Ghorbani, M. A., Chau, K.-W., & Kazem Pour, R. (2018). Novel genetic-based negative correlation learning for estimating soil temperature. *Engineering Applications of Computational Fluid Mechanics*, *12*(1), 506–516.
Krieger, I. M., & Dougherty, T. J. (1959). A mechanism for non-Newtonian flow in suspensions of rigid spheres. *Transactions of the Society of Rheology*, *3*(1), 137–152.
Kulkarni, D. P., Das, D. K., & Vajjha, R. S. (2009). Application of nanofluids in heating buildings and reducing pollution. *Applied Energy*, *86*(12), 2566–2573.
Kurt, H., & Kayfeci, M. (2009). Prediction of thermal conductivity of ethylene glycol–water solutions by using artificial neural networks. *Applied Energy*, *86*(10), 2244–2248.
Lee, S., Choi, S. U.-S., Li, S., & Eastman, J. A. (1999). Measuring thermal conductivity of fluids containing oxide nanoparticles. *Journal of Heat Transfer*, *121*(2), 280–289.
Lee, J.-H., Hwang, K. S., Jang, S. P., Lee, B. H., Kim, J. H., Choi, S. U. S., & Choi, C. J. (2008). Effective viscosities and thermal conductivities of aqueous nanofluids containing low volume concentrations of Al_2O_3 nanoparticles. *International Journal of Heat and Mass Transfer*, *51*(11–12), 2651–2656.
Lee, S. W., Park, S. D., Kang, S., Bang, I. C., & Kim, J. H. (2011). Investigation of viscosity and thermal conductivity of SiC nanofluids for heat transfer applications. *International Journal of Heat and Mass Transfer*, *54*(1–3), 433–438.
Li, H., Zhang, Z., & Liu, Z. (2017). Application of artificial neural networks for catalysis: A review. *Catalysts*, *7*(10), 306.
Loni, R., Asli-Ardeh, E. A., Ghobadian, B., Ahmadi, M. H., & Bellos, E. (2018). GMDH modeling and experimental investigation of thermal performance enhancement of hemispherical cavity receiver using MWCNT/oil nanofluid. *Solar Energy*, *171*, 790–803.
Maïga, S. E. B., Nguyen, C. T., Galanis, N., & Roy, G. (2004). Heat transfer behaviours of nanofluids in a uniformly heated tube. *Superlattices and Microstructures*, *35*(3), 543–557.
Mahbubul, I., Saidur, R., & Amalina, M. A. (2012). Latest developments on the viscosity of nanofluids. *International Journal of Heat and Mass Transfer*, *55*(4), 874–885.
Masuda, H., Ebata, A., & Teramae, K. (1993). Alteration of thermal conductivity and viscosity of liquid by dispersing ultra-fine particles. Dispersion of Al_2O_3, SiO_2 and TiO_2 ultra-fine particles. *Netsu Bussei*, *7*(4), 227–233.
Mehrabi, M., Sharifpur, M., & Meyer, J. P. (2013). Viscosity of nanofluids based on an artificial intelligence model. *International Communications in Heat and Mass Transfer*, *43*, 16–21.
Meybodi, M. K., Daryasafar, A., Koochi, M. M., Moghadasi, J., Meybodi, R. B., & Ghahfarokhi, A. K. (2016). A novel correlation approach for viscosity prediction of water based nanofluids of Al_2O_3, TiO_2, SiO_2 and CuO. *Journal of the Taiwan Institute of Chemical Engineers*, *58*, 19–27.
Meybodi, M. K., Naseri, S., Shokrollahi, A., & Daryasafar, A. (2015). Prediction of viscosity of water-based Al_2O_3, TiO_2, SiO_2, and CuO nanofluids using a reliable approach. *Chemometrics and Intelligent Laboratory Systems*, *149*, 60–69.
Meyer, J. P., Nwosu, P. N., Sharifpur, M., & Ntumba, T. (2012). Parametric analysis of effective viscosity models for nanofluids. In ASME 2012 International Mechanical Engineering Congress and Exposition, vol. 7, 1149–1157. New York: American Society of Mechanical Engineers.
Murshed, S., Leong, K. C., & Yang, C. (2008). Investigations of thermal conductivity and viscosity of nanofluids. *International Journal of Thermal Sciences*, *47*(5), 560–568.
Naik, M., & Sundar, L. S. (2011). Investigation into thermophysical properties of glycol based CuO nanofluid for heat transfer applications. *World Academy of Science, Engineering and Technology*, *59*, 440–446.
Namburu, P. K., Kulkarni, D. P., Misra, D., & Das, D. K. (2007). Viscosity of copper oxide nanoparticles dispersed in ethylene glycol and water mixture. *Experimental Thermal and Fluid Science*, *32*(2), 397–402.
Nguyen, C., Desgranges, F., Roy, G., Galanis, N., Maré, T., Boucher, S., & Angue Mintsa, H. (2007). Temperature and particle-size dependent viscosity data for water-based nanofluids–hysteresis phenomenon. *International Journal of Heat and Fluid Flow*, *28*(6), 1492–1506.
Nielsen, L. E. (1970). Generalized equation for the elastic moduli of composite materials. *Journal of Applied Physics*, *41*(11), 4626–4627.
Pak, B. C., & Cho, Y. I. (1998). Hydrodynamic and heat transfer study of dispersed fluids with submicron metallic oxide particles. *Experimental Heat Transfer an International Journal*, *11*(2), 151–170.
Papari, M. M., Yousefi, F., Moghadasi, J., Karimi, H., & Campo, A. (2011). Modeling thermal conductivity augmentation of nanofluids using diffusion neural networks. *International Journal of Thermal Sciences*, *50*(1), 44–52.
Pastoriza-Gallego, M., Casanova, C., Legido, J. L., & Piñeiro, M. M. (2011). CuO in water nanofluid: Influence of particle size and polydispersity on volumetric behaviour and viscosity. *Fluid Phase Equilibria*, *300*(1–2), 188–196.
Pourkiaei, S. M., Ahmadi, M. H., & Hasheminejad, S. M. (2016). Modeling and experimental verification of a 25W fabricated PEM fuel cell by parametric and GMDH-type neural network. *Mechanics & Industry*, *17*(1), 105.
Rudyak, V. Y., Belkin, A. A., & Egorov, V. V. (2009). On the effective viscosity of nanosuspensions. *Technical Physics*, *54*(8), 1102–1109.
Rudyak, V. Y., Dimov, S. V., & Kuznetsov, V. V. (2013). On the dependence of the viscosity coefficient of nanofluids on particle size and temperature. *Technical Physics Letters*, *39*(9), 779–782.
Rudyak, V. Y., & Krasnolutskii, S. (2014). Dependence of the viscosity of nanofluids on nanoparticle size and material. *Physics Letters A*, *378*(26–27), 1845–1849.
Shaikh, S., Lafdi, K., & Ponnappan, R. (2007). Thermal conductivity improvement in carbon nanoparticle doped PAO oil: An experimental study. *Journal of Applied Physics*, *101*(6), 064302.

Singh, M., & Kundan, L. (2013). Experimental study on thermal conductivity and viscosity of Al_2O_3-nanotransformer oil. *International Journal on Theoretical and Applied Research in Mechanical Engineering*, *2*(3), 2319–3182.

Takagi, T., & Sugeno, M. (1985). Fuzzy identification of systems and its applications to modeling and control. Readings in fuzzy sets for intelligent systems. *IEEE transactions on systems, man, and cybernetics*, *1*, 116–132.

Taormina, R., Chau, K.-W., & Sivakumar, B. (2015). Neural network river forecasting through baseflow separation and binary-coded swarm optimization. *Journal of Hydrology*, *529*, 1788–1797.

Tavman, I., Turgut, A., Chirtoc, M., Schuchmann, H. P., & Tavman, S. (2008). Experimental investigation of viscosity and thermal conductivity of suspensions containing nano-sized ceramic particles. *Archives of Materials Science*, *34*(2), 99–104.

Wu, C., & Chau, K. (2011). Rainfall–runoff modeling using artificial neural network coupled with singular spectrum analysis. *Journal of Hydrology*, *399*(3–4), 394–409.

Yousefi, F., Karimi, H., & Papari, M. M. (2012). Modeling viscosity of nanofluids using diffusional neural networks. *Journal of Molecular Liquids*, *175*, 85–90.

Zhang, S., & Chau, K.-W. (2009). Dimension reduction using semi-supervised locally linear embedding for plant leaf classification. In D.-S. Huang, K.-H. Jo, H.-H. Lee, H.-J. Kang, & V. Bevilacqua (eds.), *Emerging intelligent computing technology and applications: 5th International Conference on Intelligent Computing, ICIC 2009, Ulsan, South Korea, September 16–19, 2009. Proceedings*, pp. 948–955. Berlin: Springer.

Zhang, Z., Li, H., Chang, H., Pan, Z., & Luo, X. (2018). Machine learning predictive framework for CO_2 thermodynamic properties in solution. *Journal of CO_2 Utilization*, *26*, 152–159.

Zhao, J.-F., Luo, Z.-Y., Ni, M.-J., & Cen, K.-F. (2009). Dependence of nanofluid viscosity on particle size and pH value. *Chinese Physics Letters*, *26*(6), 066202.

Zhou, S.-Q., Ni, R., & Funfschilling, D. (2010). Effects of shear rate and temperature on viscosity of alumina polyalphaolefins nanofluids. *Journal of Applied Physics*, *107*(5), 054317.